ANIONIC EFFECTS IN HOT SURFACE CATALYZED COMBUSTIONS

William Bannister,[1,2,*] Fang Lai,[1,3] Weera Paramasawat,[3] Wipoo Sriseubsai,[3] Alfred Donatelli,[14] Jun Li,[2] Francis Bonner,[4] Nick Schott,[3] Pradeep Kurup,[5] James Egan,[6] Edwin Jahngen,[2] Pongphisanu Muangchareon,[4] Nukul Euaphantasate,[7] ShihKun Chiang,[2] S. K. Sengupta,[2] C-S Kuo,[8] Ramaswamy Nagarajan,[1] Jirayu Chaospukhum,[2] Apisak Meesrisom,[2] Vinit Kongkadee,[2] Vytenis Babrauskas[11]

Univ. of Massachusetts–Lowell, Lowell, MA 01854: [1]Center for Fire Research; [2]Chemistry Dept; [3]Plastics Engineering Dept; [4]Chemical Engineering Dept; [5]Civil & Environmental Engineering Dept.; [6]Physics Dept. [7]Nat'lMetal & Materials Tech.Ctr, 114 Thailand Science Park, Paholyothin Rd. Klong 1, Klong Luang, Pathumtani 12129, Thailand. [8]Nat'l Cheng Kung Univ, Tainan, Taiwan, Materials Science & Engineering Dept. [9]Univ.of Maryland, Mechanical Engineering Dept. [10]Arizona State Univ. Mechanical & Aeronautical Engineering Dept. [11]Fire Science & Technology Inc.,9000 – 309th Place SE, Issaquah WA 98027

[*]To whom correspondence should be addressed: E-mail: William_Bannister@uml.edu

Initial phases of hot surface catalyzed hydrocarbon oxidation are anionic, and not free radical in character. Anionic oxygen species such as the radical anion abstract a proton to form caged carbanion/hydroxyl free radicals. Hydrocarbon free radical character then arises by electron transfer from the hydrocarbon carbanion to the caged hydroxyl radical. The formation of the carbanion determines the ultimate course of the overall oxidation reaction. Correlations regarding ignition temperatures and hydrocarbon oxidation product identity are consistent with carbanionic but not free radical effects. Thus, highly polarized surfaces (e.g., quartz and corroded surfaces), and addition of polar compounds to fuel/air mixtures facilitate ignitions. Isotope, ignition temperatures and combustion trends are consistent with Seebeck effects (ease of electron migration in unevenly heated areas). Electrostatic Force Microscopy confirms increased electrostatic intensities at microscopic surface defects. Transient rapidly moving incandescent "red spots" often appear to presage imminent outbreak of ignition across the surface fuel impinging on hot surfaces. Negative electrostatic charge effects facilitate hot surface catalyzed oxidations. There is an inverse relationship between hydrocarbon ignitability and combustibility, with regard to hot surface effects. Seebeck effects govern the adsorption and availability of oxygen radical anions at the hot surface, and overall Seebeck effects are the most important in initiation and control of combustion and fire. Surfaces with negative Seebeck effects more easily inspire selective oxidations, by draining electron density from developing hot spots and thus requiring higher temperatures to effect ignition of impinged hydrocarbon fuels than is the case for positive Seebeck effect surfaces. Increases in negative electrostatic field strength appear to be associated with combustibility.

General

In selective (flameless) oxidations of hydrocarbons, C-H bonds rupture with insertion or addition of oxygen species to form combustion products. In total oxidation (with or without flame), the hydrocarbon is completely oxidized to CO_2 and water. [1] Fuel flammability indices include flash points (the minimum temperatures for liquid fuels to sustain sufficient vapor concentrations in air to produce ignition when an open flame is passed over the surface); and hot surface ignition, or autoignition temperature [AIT] (with no open flame for a surface in contact with a given fuel causing "self-sustained combustion".[2] Currently accepted hydrocarbon oxidation

mechanisms involve free radical attack by oxygen species such as the atomic oxygen radical anion below) on C-H bonds, to yield propagating alkyl free radicals and hydroxide ion; see (Equation 1): [3, 4]

$$R-H + {^-}:\ddot{O}\cdot \rightarrow R\cdot + {^-}:\ddot{O}-H \tag{1}$$

AIT determinations are subject to test methods. In recent videotaped comparisons[5] of previously cited AIT values of 240° C [(6) for JP4 fuel with that of the much less volatile JP8, the same AIT was observed for both fuels but at a much higher temperature $(540 \pm 20^o$ C). Several previously unidentified features were noted; see Figure 1. After application of fuel drops onto a hot stainless steel surface, a dark envelope expanded outward, with wisps of smoke. Red-hot incandescent spots moved rapidly over the surface outward from this dark patch, at heating temperatures as low as 380° C, although red incandescence of iron typically occurs above 525° C. [7] These incandescent events can last many seconds before actual flame formation occurs. (Other workers have also observed pre-flame "red spots". [8,9] Blue "cool" flames were often observed at the outer edges of the red spots, with almost immediate transformation of these flickering blue flames to a sheet of white-hot flame over the entire test area. The following sequence of events is speculated:

1. The fuel drop vaporizes, cooling the immediate impact area of the hot surface. Fuel concentrations within the cloud are initially above the upper flammability limit. [10]

2. Within the fuel cloud there is initial flameless oxidization, forming CO, CO_2, and water and further reducing O_2 levels. Heating causes thermal eddies and convection currents, effecting isolated contiguous hotter and cooler surface areas. Within hotter areas oxidation rates are enhanced to the extent that there can be momentary attainment of an incandescent "red spot", flickering and moving around as a result of convection currents.

3. For "red spots" at the periphery of the fuel cloud, where oxygen levels are higher in contiguous cooler areas (but still hot enough to sustain ignition), the fuel/air mixture may be lean enough to afford ribbons of blue carbon monoxide flame" along this periphery, which suddenly transform to a sheet of white hot flame over the entire surface.

Other workers have shown that combustion occurs prior to flaming combustion, with CO and CO_2 being prominent products; see Table 1. [11]

Table 1. Oxidation of 9% CH_4/air at $1050\,^o$C (about $500\,^o$C below maximum IT)

Gas Present	With Pt^o bar, %	With Ni^o bar, %
Natural gas, at start	9.1	8.99
CO_2, after 8 minutes	1.01	0.05
CO, after 8 minutes	0.72	0.50
Natural gas, at start	8.75	8.77
CO_2, after 20 minutes	1.96	0.07
CO, after 20 minutes	0.22	0.36

The observed AIT of 540° C for both JP4 and JP8 can be attributed to CO formation, with an AIT somewhat higher (609° C). The transient incandescent red spots do not persist long enough for true temperature registration, but would be hot enough for CO ignition. Also, the range of lower to upper flammability limit [10] is much greater for carbon monoxide (12.5% to 74%, ideal for a fuel rich environment) than for alkane fuels (e.g., hexane, with very narrow ranges of 1.1% to 7% [2]. Thus, AIT determinations may pertain not to the substrate being measured, but rather to decomposition products such as carbon monoxide.

This suggests that the first pre-flame phase is a relatively low energy selective process. As will be discussed, we believe adsorbed oxygen radical anions thermally react as strong Lewis bases with the hydrocarbon C-H bonds to form carbanionic incipient intermediates. These then undergo electron transfer to form corresponding hydrocarbon free radicals, and proceed through previously documented mechanistic pathways to form selective and total oxidations products. As oxidation ensues with rising temperatures, the rate of formation of the free radical population also increases. When the rate of free radical propagation exceeds the rate of flameless free radical depopulation processes, runaway flame chemistry ensues.
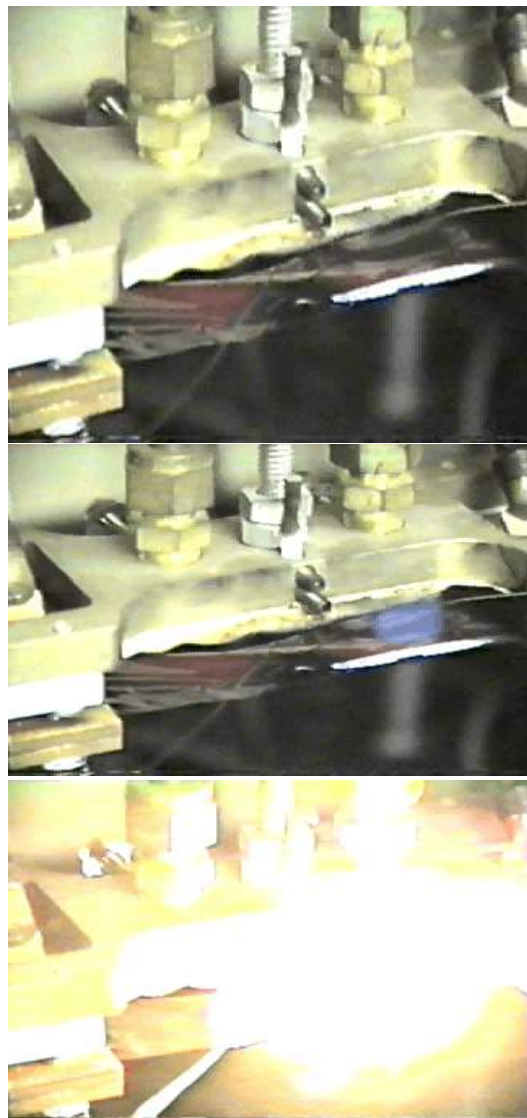

Fig. 1. Hot Surface Precombustion, flameless Combustion and Ignition: JP-4 on stainless steel steel surface at 380° C.

Fuel droplet vaporizes on hot surface (*ca*. 380°C. Hemispherical fuel rich cloud of vapor expands outward, with some smoke. Low molecular weight decomposition products (CO, etc.) diffuse rapidly to periphery of fuel cloud. Decomposition raises local surface temperatures to above 520°C, incandescent red hot spots fleeting over the steel surface.

As surface temperatures increase to 540°C, blue flames attributable to formation and combustion of CO [12] flicker at the outer periphery of the red spots.
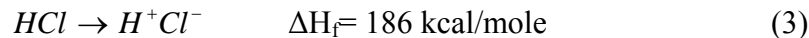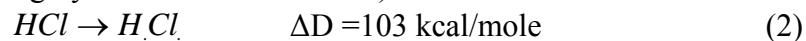
Sudden transformation of blue flame to "hot" flame over entire test area.
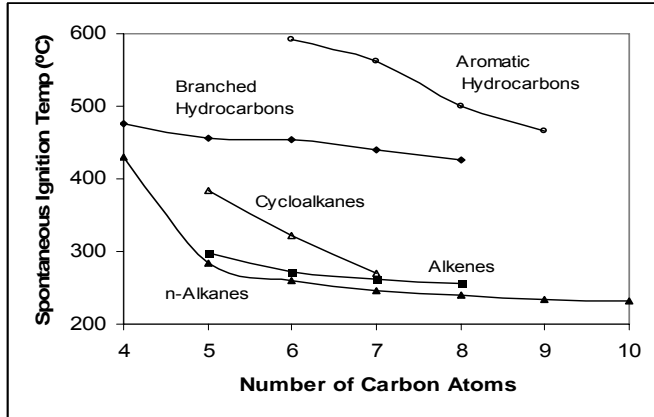
Fig.2. Fuel Characteristics. AIT values for various hydrocarbons families [10]. These AIT trends are exactly opposite to trends involving free radical reaction proclivities for these species. [13 – 15].

GENERAL CONSIDERATIONS: ANIONIC VS. FREE RADICAL MECHANISMS

Fire reactions are commonly considered to be in the gas phase, and it is true that free radical (and positively charged cationic) reactions tend to proceed with much less energy reqirements than is the case for ionic reactions in the gas phase. [15] However, pre-flame combustion reactions take place by interaction with oxygen species adssorbed onto the solid phase surface of a hot target; and gas phase arguments are not applicable. For example, the gas phase free radical process is favored for the free radical reaction (2) over the ionic gas phase dissociation (3) of HCl [15] (both being highly endothermic reactions):

$$HCl \rightarrow H \cdot Cl \cdot \qquad \Delta D = 103 \text{ kcal/mole} \qquad (2)$$

$$HCl \rightarrow H^+ Cl^- \qquad \Delta H_f = 186 \text{ kcal/mole} \qquad (3)$$

On the other hand, impingement of gaseous HCl onto a basic solid surface such as NaOH obviously results in an exothermic ionization process.

POLARITY IN AMBIENT AIR EFFECTS

In studies of mixtures of hydrocarbon gases with halons, hydrogen bromide, and water (all highly efficient polar fire extinguishing agents which appreciably polarize ambient air in the vicinity of hot surfaces), it was found that instead of inhibiting ignition, these actually were ignition promoters! [16,17,18] These results provide further argument for a polar rather than a free radical pathway in facilitating ionic ignition initiation processes in surface ignitions.

HOT SURFACE CHARACTERISTICS.
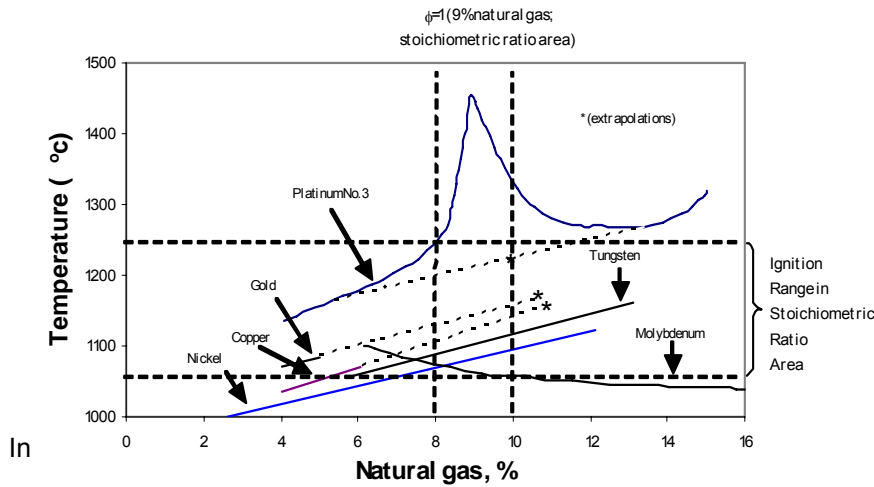
Fig.3. Natural gas ignition on hot metal surfaces, with flameless combustion below the AIT values. [11] "The sharp maximum in temperature for Pt^o is an artifact caused by transient surface heating as ignition occurs" [19]. (This is reminiscent of the "red spot" observations described on pages 2-3 and in Figure 1.)

In heated metal surfaces with varying surface temperatures there are electrical charge effects with polarizing influences in these different zones. Seebeck effects induce charge transfers in heated metals, the polarity and magnitude of these depending on the metal. Many ("n-type") metals exhibit a negative Seebeck effect, with a diffusion of electron density toward the cooler side, and a corresponding partially negatively charged character at the cooler side. For positive "p-type" metals (such as tungsten, molybdenum, copper, gold and silver), there is a reversed electron diffusion from cooler to hotter metal surfaces, and a corresponding positively charged polarization at the cooler end.. [20-25] (See Figure 4.)

Note: In the context of Figure 4, the "hot" end in the system is the driving heat source, and the "cool" end is the combustion surface on which the actual "hot surface combustion" takes place. Thus, as temperatures rise on the cooler surfaces during combustion for the "n-type" metals, this surface becomes *less* negatively charged as there is a relative migration of electron density back to the hotter end. It will be shown that combustion is dependent on negative charge character, and therefore combustion tendencies on such n-type metals will require hotter and hotter temperatures; thus, n-type metals are self controlling with regard to ignition. Likewise, for the "p-type" metals the negative charge character at the combustion surface will *increase* during combustion, thus requiring lower temperatures for ignition to take place. As temperatures rise due to pre-ignition combustion effects, the electron densities at the surface become higher and higher, with runaway ignition then transpiring. Thus, "n-type" metals would be expected to have higher ignition temperature, and "p-type" metals would have lower ignition temperatures. (See Figure 5.)

5

Hot

+

Voltage

-

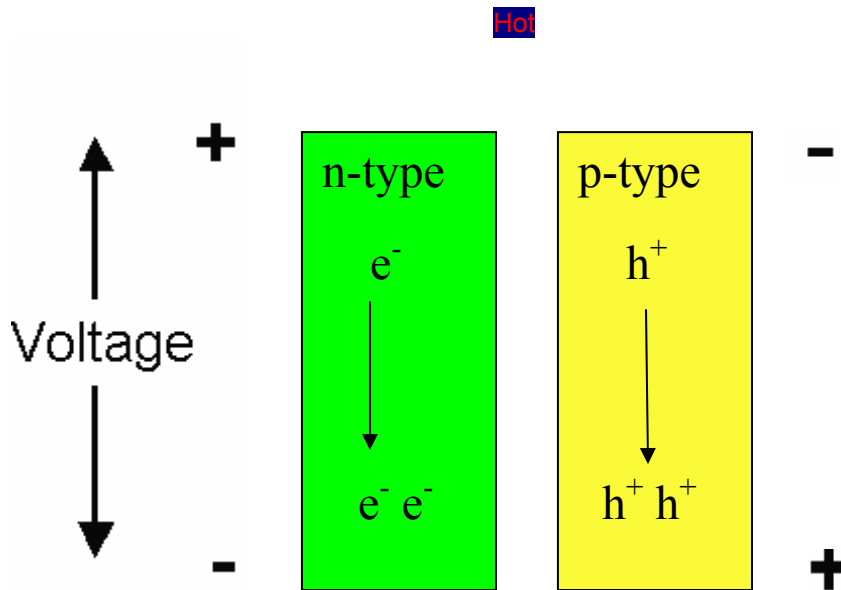n-type

e⁻

e⁻ e⁻

p-type

h⁺

h⁺ h⁺

-

+

Cold

Fig.4. Polarization by Seebeck effect for negative n-type (e.g., Ti, Pt, Ni, and Pd) and positive p-type coefficient metals (e.g. W, Mo, Cu, Ag, Au). [25]
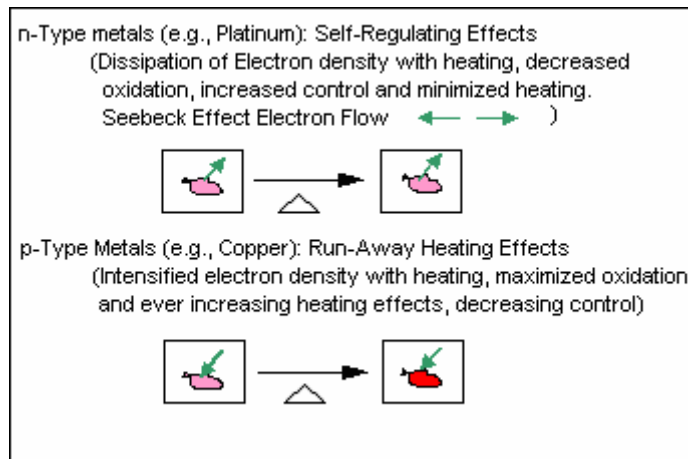
n-Type metals (e.g., Platinum): Self-Regulating Effects
(Dissipation of Electron density with heating, decreased oxidation, increased control and minimized heating.
Seebeck Effect Electron Flow   ◄— —►   )

p-Type Metals (e.g., Copper): Run-Away Heating Effects
(Intensified electron density with heating, maximized oxidation and ever increasing heating effects, decreasing control)

Figure 5.   Inverse correlation of Seebeck effects and ignition temperatures.

   In Table 2 and its accompanying data plot, there is an apparent correlation of Seebeck effects with combustibility, at least for the six metals (tungsten, molybdenum, copper, gold, platinum and nickel) for which there are both ignition and Seebeck data, in terms of ignitability trends for given hydrocarbon fuels in contact with various *n*-type and *p*-type metals. There appear to be two families, comprised of metals which don't form oxides, and for which decreasing ignition temperatures would be predicted for increasing Seebeck coefficients; and oxidizable metals, for which evidence will be discussed in the next section for relatively reduced temperature effects.

Table 2. Thermoelectric Power and Ignition Proclivity for Combustion Catalysts

	Metal	AIT (°C) @ Φ = 1 (see Fig. 3)	Seebeck coefficientt (µv/°C) @ AIT [20]	M.P. (°C) [26]	Oxidation Comments [27]
P –type	W	1050	+18	3410	Stable to aerial oxidation.
	Mo	1075	+17	2617	”
	Ag	--	+8 to +10	962	Oxidizes at lower temperatures; some but probably not total reversion to metal in AIT range.
	Cu	1000	8	1083	”
	Stainless steel	--	+3 to +4 [28]	1427	Stable to aerial oxidation
N - type	Au	1150	-3.9	1064	”
	Ti		-5 to - 2	1650	”
	Pt	1450	-21.5	1772	”
	Ni*	1070	-30	1453	Oxidizes at lower temperatures; oxide is stable in AIT range.
	Pd	--	-31 to -34	1552	Stable to aerial oxidation.

Notes: AIT : Autoignition temperature
Φ = 1: Stoichiometric ratio for complete combustion of natural gas (methane 97%, ethane 3%).
-- : AIT under these conditions not yes determined; ranking is in terms of predicted AIT value.
 * Nickel is anomalous due to oxide formation; see comments below.

Table 2. Thermoelectric Power and Ignition Proclivity for Combustion Catalysts
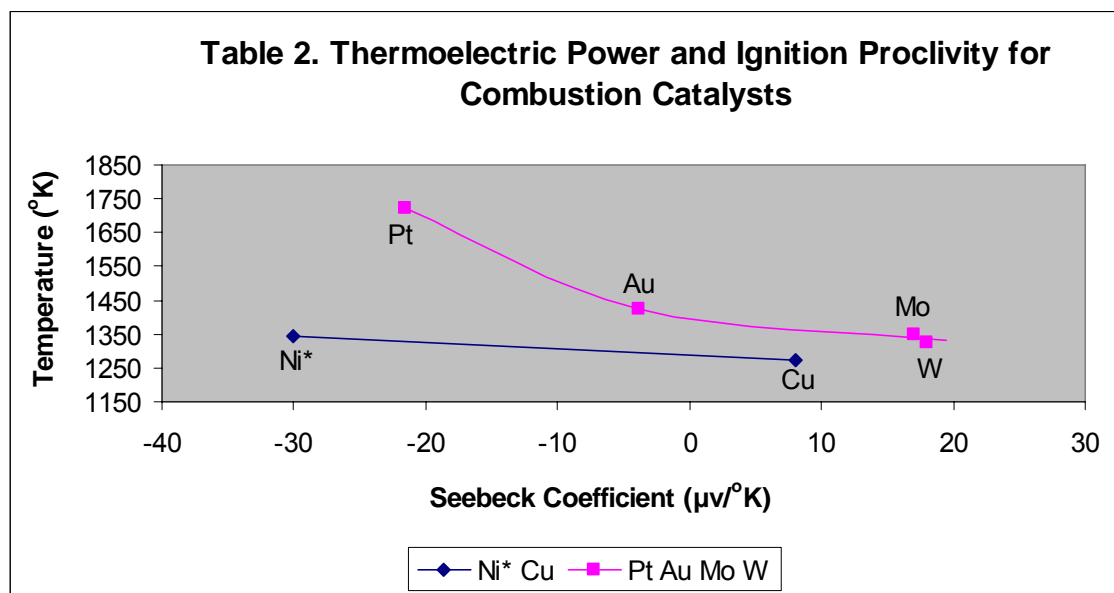
OXYANIONIC AND CORRODED SURFACE EFFECTS

As noted above, there is an apparent negative electrostatic character to be associated with facilitation of combustion. Although quartz is non-metallic with no Seebeck effect, and typically no significant surface defects (see discussion below), it is an efficient ignition source with low ignition temperatures *(2)*. This may be due to the strong polarization of adsorbed oxygen molecules, due to the high partial negative charge of the oxygen species which comprise the entire

surface of the silicate matrix (see Figure 6) *(29)*. It would be anticipated that the partial negative charge character would increase with increasing temperatures, due to the thermal weakening of the silicon-oxygen bonding. Thus, the same "runaway" would exist here as with the p-type metal situations, in which localized heating in incandescent red spots would result in ever increasing negative charge character and ever increasing runaway combustion rates. Similar considerations can be made for other oxidized surfaces, such as nickel oxide and iron rust, also excellent ignition sources *(30,31,32)*. Unlike quartz and similar materials with very smooth surfaces, corroded metal surfaces will have particularly very high concentrations of electrostatic charges mounted at the promontories the surface defects of such surfaces; see discussions in the next section.   There have been findings of "p-type" character of oxides of metals such as nickel, for which the metal itself possesses "n-type" character. This would serve also to reduce ignition temperatures *(33)*.
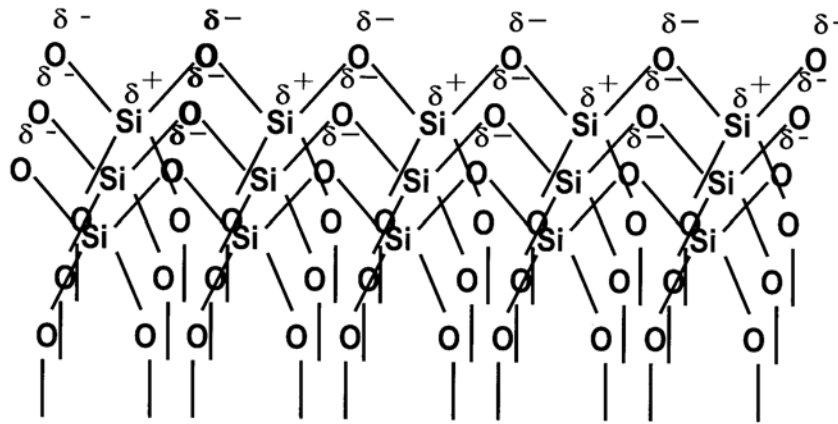
Fig. 6.   Polarization of quartz, glass and similar silica surfaces, with charge densities due to electro negativities: Si, 40% positive; O, 20% negative.[33]

ELECTROSTATIC FIELD EFFECTS ARISING FROM SURFACE MICRODEFECTS.

The magnitude of Seebeck coefficient charge effects (typically microvolts/^{o}C change in temperature) may appear to be very small, but microscopically all surfaces are entirely covered by considerable defects in terms of terraces, steps, ledges, and kinks and similar elevated features (see Figure 7). [30-32]
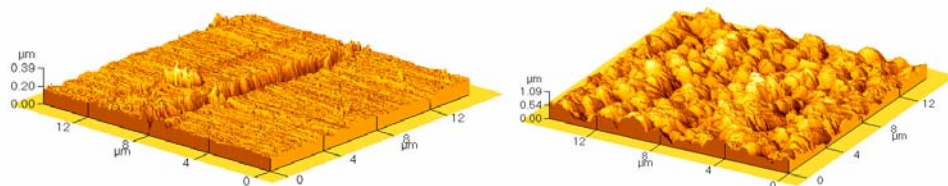
Fig. 7. AFM images of polished sterling silver (left), and of the same sample (right) with oxidized surface.

Increased catalytic activity and electrical effects at the tips or edges of such features have also been observed. [29,30] Since the area of these tips is very small in comparison to the total surface area, there is accordingly a drastic increase in density of these localized charges.[34] An

inference can then be drawn from this effect in terms of surface microdefects at a hot surface (with a hotter heat source driving a heat flow and Seebeck electron drift to or from this surface).

EXPERIMENTAL RESULTS

1. ATOMIC FORCE AND ELECTROSTATIC FORCE MICROSCOPY (AFM/EFM)

AFM examinations at surfaces exhibit uneven landscapes characterized by valleys with surrounding steppes, shelves, cliffs, spires and crags. EFM experiments were performed to show that polar effects in hot surface ignitions may be initiated at select pinpoint areas of the surface, where electrostatic effects are intensified due to localized micro surface defect character and localized energizing. EFM measures spatial variation of surface charge carriers at the microscopic level, mapping surface charges, dielectric constants and electrical potentials on surfaces, as can be generated by the Seebeck effect and resulting polarizations of adsorbed oxygen on hot surfaces *(35)*. Several metals (Ni, Mo, and Pt) were studied to measure relative surface potentials simultaneously with topography, focusing on DC probe tip bias voltage changes with different surface potentials at room temperature. No temperature gradient was imposed; thus no Seebeck effects were involved. The AFM/EFM results for nickel for various imposed surface voltages are shown in Figures 8 a-d; similar results pertained for the other metals. The contrast of features in EFM is related to the electrostatic strength between the probe tip and sample. The AFM signal in each case reveals numerous promontories due to surface imperfections, at which electrostatic charge intensities are concentrated. With a positively charged probe tip and negatively charged sample, the attractive force between the unlike charges show up as brighter portions of the image, being concentrated at these surface peaks. The EFM voltage is relative to the strength of electrostatic interaction between the tip and the sample. Conversely, when both probe tip and sample are positively charged, repulsive forces between the like charges show up as darker portions. It can be reasoned that polar effects in hot surface ignitions are initiated at select pinpoint areas of the surface, wherein electrostatic effects are particularly exacerbated due to the localized micro surface defect character and localized energizing.


a. AFM topography.   b.EFM, +5 volts   c. EFM, 0 volts   d. -5 volts
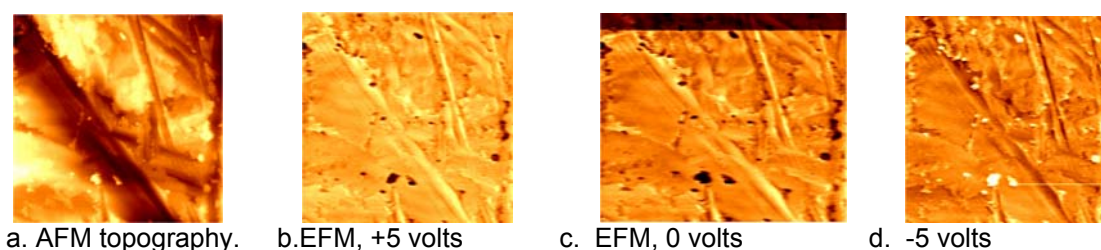
Fig. 8.   AFM and EFM views of polished nickel surface at various applied voltage

levels. (Constant temperature, 25° C; no Seebeck effect.)

**2. NEGATIVE ELECTROSTATIC CHARGE ENHANCEMENT OF OXIDATION**

Wide ranges of methane/air and butadiene/air mixtures were exposed to catalytic surfaces at temperatures of 500 - 600° C and with both positive and negative electrostatic charges being applied to the surfaces, using a combustion apparatus shown in Figure 9. In typical experiments flow rates of 50 mL/minute of methane and 25 mL/minute of air were combined and fed through

a one-meter length of 8 mm (ID) type 301 stainless steel tube held in a Lindberg furnace. (Air was thus the limiting reagent, with perhaps $7x10^{-3}$ moles of oxygen available during the course of a typical 25-minute run.)
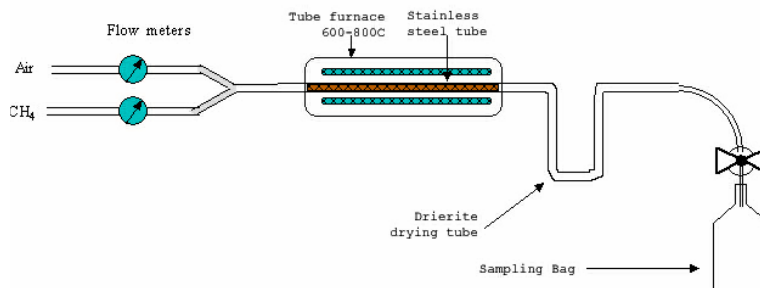

**Fig. 9.   Combustion apparatus.**

Electrostatic charges of zero, -5 kV and +5 kV magnitudes were successively applied to the metal combustion tube. One-liter Tevlar™ sample bags were filled with the effluent combustion gases after preliminary drying with conventional Drierite™ or Anhydrite™.   Analytical determinations by our group were limited to gas concentrations of carbon monoxide, using an Extech Instruments Corp. Model C050 carbon monoxide meter; gravimetric attempts to determine CO_2 and H_2O were inconclusive due to difficulties imposed by the relatively small masses of these product gases which were evolved during the course of the experiments. A total of five determinations were performed on contract by IMR Environmental Equipment Inc. of St. Petersburg, FL for residual oxygen and for carbon monoxide and carbon dioxide
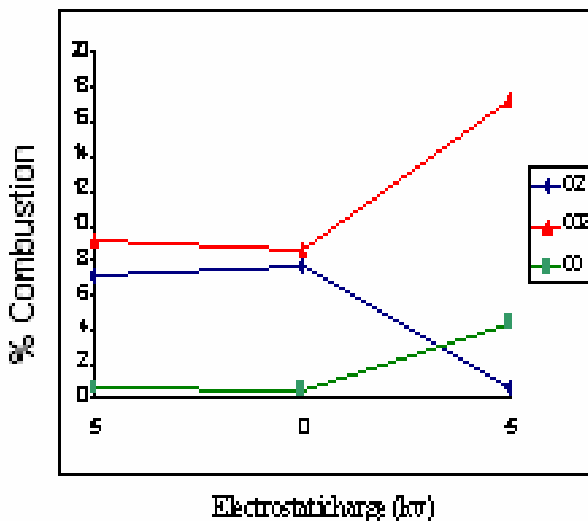
Fig. 10. Preliminary results of oxidation of a fuel-rich mixture of methane and air in a stainless steel tube at 650°C: per cent combustion *vs.* kilovolt electrostatic surface charge.   (Negative charges appear to enhance oxidation.) [Results reported by IMR Environmental Equipment Inc.]
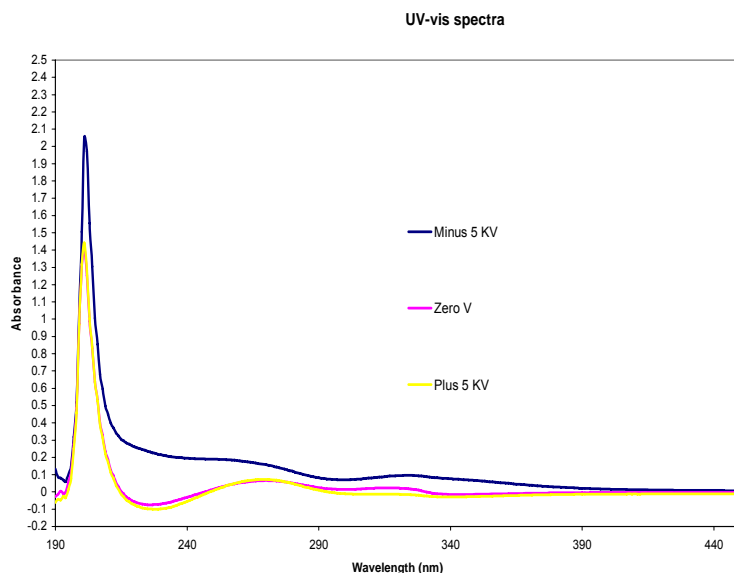
UV-vis spectra

Fig.11 UV-vis spectra: effects of +/- electrostatic field applications on hot surface catalyzed oxidation of butadiene to form maleic anhydride: facilitation by negative charge application.
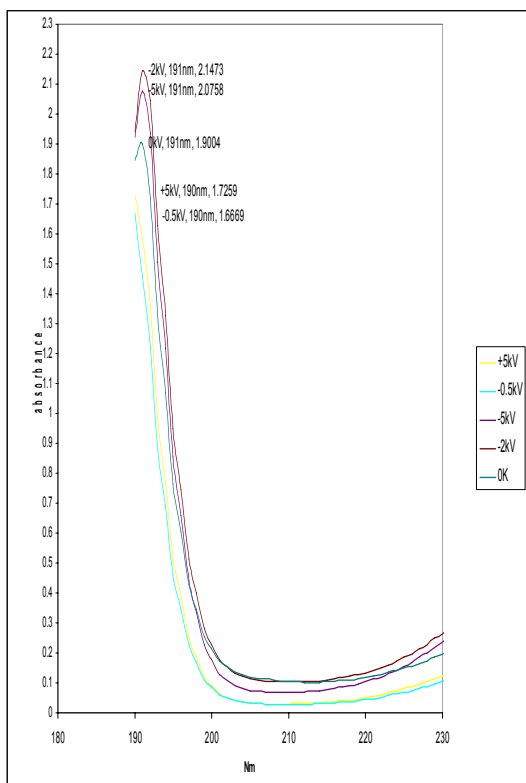
Fig. 12 UV spectra of aqueous solutions of vapor products from hot surface catalyzed oxidations of butadiene to form 3,4-epoxy-1-butene: facilitation by negative charge application. (The accepted UV absorption for maleic anhydride is 20 7 nm. The observed absorption at 191 nm corresponds to formation of the monoepoxide [3,4-epoxy-1-butene]. If this is the case, this may be an instance in which it may product identity may be effected electrostatically.

Experimental conditions: 42" stainless steel (#306) Tubing (O.D. = 0.25"). Flow rate of gas stream comprised of 10 mL /minute butadiene and 60 mL dry air/minute Temperature: 450° C. Observed value of absorbance of 1.7259 at 5 kV was for an enriched sample obtained by combination of two 20-minute experimental runs. The absorbance for a comparable 20-minute run would be expected to be substantially lower.

11

products. That company's results for CO were generally consistent with our own. Butadiene was similarly subjected to hot surface oxidation. Maleic anhydride formation was anticipated [40] and indeed was observed in three of the four experiments, using uv-visible spectroscopy for product determinations. In one instance, however, formation only of 3,4-epoxy-1-butene was observed. Although both products are prepared industrially (from butane, *via* butadiene intermediacy)[41] the reaction procedures for these are quite different. This may be an instance in which it may be able to affect product identity by electrostatic control. In almost all the determinations performed by the two groups, it was observed that with negative charges, increased combustion product formations occurred, tending to confirm a relationship of negative electrostatic charge effects with hot surface induced combustion propensities; see Figures 10, 11 and 12. All of these oxidation systems appear to be facilitated by negative electrostatic charges, as has been observed in more than thirty previously performed oxidations of methane and of butadiene formulations in air, using hot stainless steel, copper, and quartz tubing.
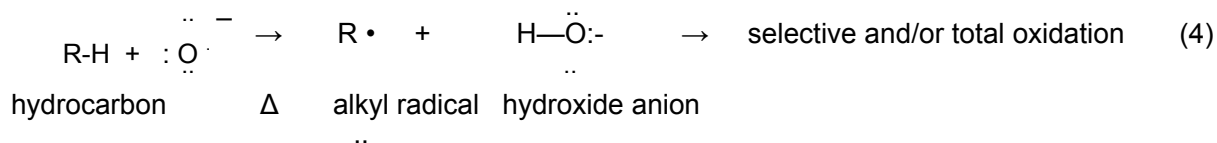
PROPOSED CARBANIONIC RATHER THAN FREE RADICAL MECHANISM

A currently accepted mechanism [36,37,38] for hot surface hydrocarbon oxidations involves a preliminary attack in which a C-H bond is severed by an attacking highly reactive species such as a hot surface energized adsorbed atomic oxygen radical anion (see Figure 13), producing two fragments. In one of these the hydrogen is transferred to the attacking species; the other is the hydrocarbon radical (less the hydrogen) remaining after the C-H bond rupture; see equation (4).

$$: \overset{..}{\underset{..}{O}} \cdot ^{-}$$

Figure 13. Atomic oxygen radical anion.

Commonly accepted free radical oxidation of hydrocarbons:

$$\text{R-H} + : \overset{..}{\underset{..}{O}} \cdot ^{-} \rightarrow \quad \text{R} \cdot \quad + \quad \text{H—}\overset{..}{\underset{..}{O}}\text{:-} \quad \rightarrow \quad \text{selective and/or total oxidation} \quad (4)$$

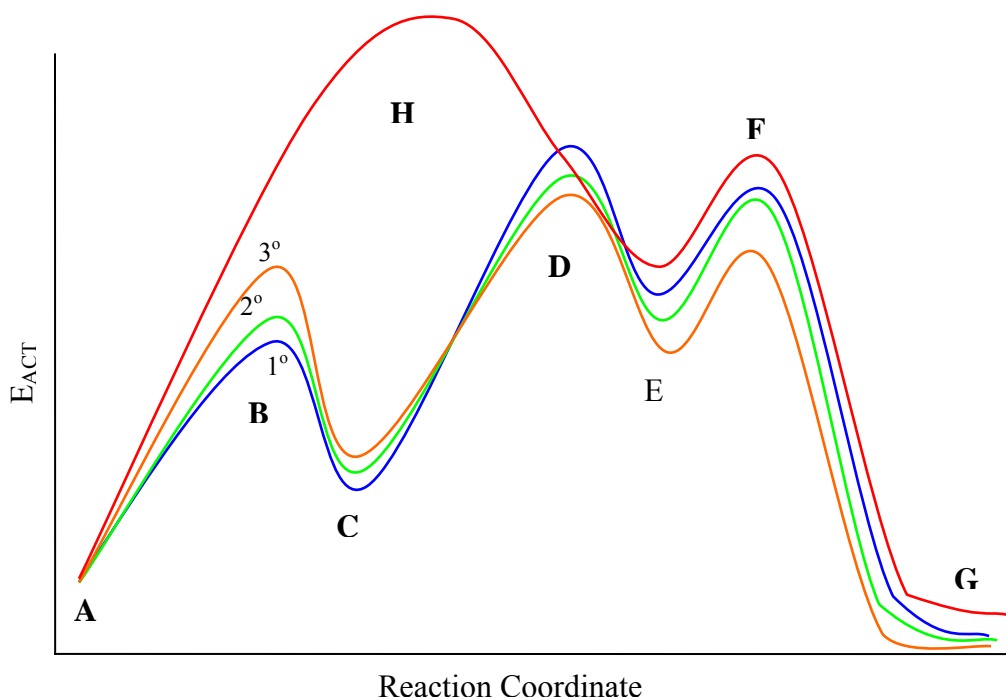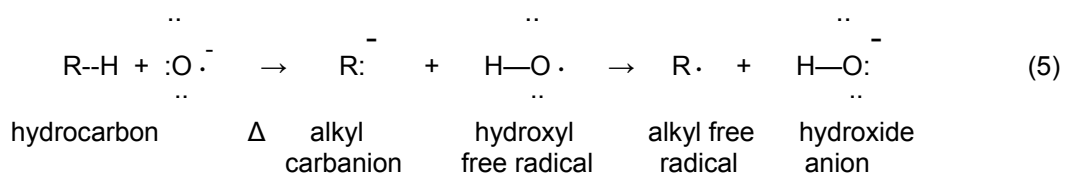hydrocarbon   Δ   alkyl radical   hydroxide anion

The atomic oxygen radical anion has three non-bonding electron pairs, and a seventh lone (free radical) electron. The three electron pairs impart strong Lewis basicity, in addition to its free radical character. In the commonly accepted theory, the O•⁻ radical anion attacks *via* its lone radical electron in a high energy rate determining reaction pathway to afford energetic propagating free radicals. These further engage in free radical propagations to yield a variety of selective oxidation products. Accompanying energy releases can result in flame oxidation. Various kinetic isotope effect studies [36,37,38] have been cited as apparent substantiation of the free radical nature of these oxidations.

From our evidence, we believe that a much lower energy initial step involves attack by the very highly basic O•⁻ radical anion, to form an alkyl carbanion and a hydroxyl free radical. In the solvated state, hydrocarbon pK_A values are about 62, but when unsolvated and at elevated temperatures these are much stronger Bronsted acids with much lower pK_A values; and in the presence of a strong base such as the unsolvated atomic oxygen radical anion adsorbed on a hot surface, an acid/base interaction would be expected to occur (*4,39*).

A high energy rate determining electron transfer from the carbanion to the hydroxyl free radical then results in an alkyl free radical and hydroxide anion.   The same products arise, but through a much lower energy and faster acid/base ionic pathway before proceeding into a slower rate determining higher energy free radical mechanism (see Figure 14. Since the reactant side of the reaction coordinate profile is comprised of the more stabilized conjugate carbocationic forms being derived from the initial ionic reaction phase, the overall isotope effect pattern would apply for either free radical and ionic pathways; and we suggest that the overall evidence favors the ionic pathway.

Proposed carbanion mechanism:

$$R\text{--}H + :\overset{..}{\underset{..}{O}}\cdot^{-} \quad \rightarrow \quad R:^{-} \quad + \quad H\text{—}\overset{..}{\underset{..}{O}}\cdot \quad \rightarrow \quad R\cdot \quad + \quad H\text{—}\overset{..}{\underset{..}{O}}:^{-} \tag{5}$$

| hydrocarbon | Δ | alkyl carbanion | hydroxyl free radical | alkyl free radical | hydroxide anion |

Fig.14. Reaction coordinate for combustion mechanism with preliminary carbanionic intermediacy.

Legend   **A:** Reactants: R-H + $:\overset{..}{\underset{..}{O}}\cdot^{-}$

Blue line	—	denotes primary hydrocarbon;
Green line	—	denotes secondary hydrocarbon;
Orange line	—	denotes tertiary hydrocarbon;
Red line	—	denotes non-ionic free radical pathway

13

B: Transition state in formation of carbanion and hydroxyl free radical

C: Unstable intermediate: formation of R:$^-$ carbanion / hydroxyl free radical pair

D: Transition state in formation of R$^{\cdot}$ free radical / hydroxide anion (rate determining)

E. Unstable intermediate: formation of R$^{\cdot}$ free radical / hydroxide anion

F. Transition state in formation of oxidation products

G. Products: CO, CO_2, H_2O, etc.

H. Reaction path without carbanion intermediacy formation in fast step.

REFERENCES.

 1. Hodnett, B. K. "Heterogeneous Catalytic Oxidation." (John Wiley & Sons, New York, 2000), p. 1.

 2. NFPA 325, "Fire Hazard Properties, Flammable Liquids, Gases & Volatile Solids". Nat'l Fire Prot. Assn. Boston, 1994), pp. 4-5.

 3. Bielanski, A.; Haber, J. "Oxygen in Catalysis" (Marcel Dekker, New York, 1991) 54.

 4. Lee, J.; Grabowski, *J. Chem. Rev*. (1992) 92, 1611-1647.

 5. US Air force Fire Research Labs, Tyndall AFB, FL (private communication).

 6. Ref. 2, p. 63.

 7. *Mechanical Engineer's Handbook* (7th ed., McGraw-Hill Book Co., New York, 1967), 4-7.

 8. Smith, K.C.; Bryner, N.P. *Combust.Sci. and Tech*. (1997), 126, 225-253.

 9. Smyth, K.C.; Bryner, N.P. *"Short-Duration Autoignition Temperature Measurements for HydrocarbonFuels"*, NISTIR 4469 (Natl. Inst. of Standards and Technology, Gaithersburg, MD, Dec, 1990), p.36.

10. Ref. 2, p. 25.

11. Coward, H.; Guest, P. *J.Am.Chem.Soc*. (1927), 49, 2479-2486.

12. Sheinson, R. S; William, F. W. "Cool Flames: Ue of the Term in Combustion Chemistry and Analytical Chemistry". *Anal. Chem*. (1974), 47(7), 1197-1198.

13. March, J. "*Advanced Organic Chemistry*", 4th ed. (McGraw-Hill Co., New York, NY, 1992), 188 , 248-254, 176, 326-327.

13. Brown, H. C.; Borkowski.   *J. Am. Chem. Soc*. (1952), 74, 1894.

14. Brown, H. C.; Brewster, J. H.; Schechter, H. *J. Am. Chem. Soc*. (1954), 76, 467. Frank, C. E.; Blackham, A. U. *Natl .Adv. Comm. Aeronaut. Technical Notes* # 3384 (1955); *Chem. Abstr*. (1955), 49, 14446e.

15. Lowry,T. H.; Richardson, K. S., *"Mechanism and Theory in Organic Chemistry"* (Harper & Row, New York, 1987); pp. 304, 407, 746-747.

16. Finnerty, A. E. "*The Physical and Chemical Mechanisms Behind Fire-Safe Fuels*." BRL-1947, Ballistic Res. Labs, Abderdeen Proving Ground, MD (1976).

17. Gann, R.G. "*Fire Suppression System Performance of Alternative Agents in Aircraft Engine and DryBay Laboratory Simulations*", NIST SP 890, (Natl. Inst. of Standards and Technology, Gaithersburg, MD, Nov. 1985), p. 61-76.

18. Hamins, A.; Borthwick, P. "Suppression of Ignition over a Heated Metal Surface". *Combustion & Flame* (1998) 112, 161-170.

19. Pfefferle, L.D.; Griffin,T.A.; Winter, M.; Crosley, D.; Dyer, M.J. *Combustion & Flame* (1989) 76, 325-8.

20. Blatt, F. J.; Schroeder, P.; Foiles, C.; Greig, D. "*Thermoelectric Power of Metals*" (Plenum Press, New York, 1976), entire book; particularly pp. 1-11; 22; 69; 144 ff.

21. Heickes,R.R., "*Thermoelectricity; Science and Engineering*" (Interscience Pub., New York, 1961), 311-322.

22. Ashcroft, N.W.; Mermin, N.D. "*Solid State Physics*" (Saunders, Philadelphia,1976), pp. 355-7.

23. Kasap, S. O. "*Principles of Electronic Materials and Devices*", 2nd ed. (McGraw-Hill Book Co., New York, 2002) pp. 278-284.

24. Harman, T. C.; Honig, J. M. "*Thermoelectric and Thermomagnetic Effects and Applications*" (McGraw-Hill Book Co., New York, 1967) pp. 47-47, 110-111

25. Snyder, G. J. "The Science and Materials Behind Thermoelectrics." http://www.its.caltech.edu/~ jsnyder/thermoelectrics/science_oage,htm.

26. Weast, R. C. ed. ""Handbook of Chemistry and Physics". (CRC Press, Boca Raton, FL, 1975).

27. "The Merck Index", 11th edition. (Merck & Co., Inc., Rahway, NJ); entries 2514; 2650; 4412; 6144; 6406; 6419; 6940; 6947; 7503; 8450; 8468.

28. Debarberis, L.; Acosta, B.; Neers, M.; McGirl, C.; Sevini, F. "Assessment of Steels Ageing by Measuring the Seebeck and Thomas Effects (STEAM)". *Proc.,15th World Conf. on Non- destructive Testing* (Rome, 15-21Oct. 2000); http://www.ndt.net/article/toc/mat.htm.

29. Considine, D. M. "van Nostrand's Encylopedia", 5th ed. (van Nostrand/Reinhold Co., New York, 1976), pp. 925-926.McCracken, D. J., "*Hydrocarbon Combustion and Physical Properties*", Ballistic Research Laboratory Report No. 1496 (Aberdeen Proving Ground, Aberdeen, MD,1970); data in entire report.

30. Heinrich, V. E.; Cox, P.A. "The Surface Science of Metal Oxides". (Cambridge University Press, London, 1004), 266.

31. Phillips, C. S.: Williams, R. J. P., "Inorganic Chemistry" (Oxford Univ. Press, New York, 1965), Vol. I, page 375.

32. Corrosion", Vol. I. Sheir, L.L., ed. (John Wiley & Sons, New York), 329.

33. Wakefield, G.; Dobson, P. J.; Foo, Y. Y., Loni, A., Simons, A., Huthison, J. L. "The fabrication and characterization of nickel oxide films and their application as contacts to

polymer/porous silicon electroluminescent devices". **1997**, Semiconduct.Sci.Technol. **12**, 1304-1309.

34. Serway, R. A.; Faughn, J. S. "College Physics", 5th ed. (Harcourt Brace College Publishers, Fort Worth, TX, 1999). Pp. 500-501.

35. Nyfenegger, R.M., Penner, R.M. "*Applied Physics Ltrs*. (1997), **A5,** 457.

36. Bielanski, A.; Haber, J. "*Oxygen in Catalysis*" (MarcelDekker, Inc., New York, 1991),46.

37. Callahan, J.L.; Desmond, M.J.; Milberger,E.E.' Blum, P.R.; Bremer, N. "*Fundamental Study of the Oxidation of Butane over Vanadium Pyrophosphate*", *J.Am.Chem.Soc*. (1985), **107**(17), 4883-4892.

38. Hodnett, B. K. *op. cit*. , 5-6.

39. Carey, F. A. "Organic Chemistry, 2nd ed. (McGraw –Hill, Inc., New York, 1992), p. 4559.

40. Reference [1], pp. 136, 139-140.

41. Rreference [1], p180.